Available online at www.sciencedirect.com
ScienceDirect
Trans. Nonferrous Met. Soc. China 29(2019) 1744−1752
Transactions of Nonferrous Metals Society of China
www.tnmsc.cn

Mechanism of MoO_2 electrodeposition from ammonium molybdate solution

Hua-zhen CAO, Cheng-jian TONG, Hui-bin ZHANG, Guo-qu ZHENG

College of Materials Science and Engineering, Zhejiang University of Technology, Hangzhou 310014, China

Received 30 November 2018; accepted 4 April 2019

Abstract: A mechanism study on MoO_2 electrodeposition from ammonium molybdate solution was presented via linear sweep voltammetry, species distribution diagram, Raman spectra, Fourier transform infrared spectrometry and X-ray diffractometry. The results show that there exist two reducible species in ammonium molybdate aqueous solution, i.e. $Mo_7O_{24}^{6-}$ and molybdenum ammonium complex. In weak acid medium without NH_4^+, an obvious reduction peak denoting the reduction of $Mo_7O_{24}^{6-}$ to molybdenum(IV) oxides emerges at around −0.7 V (vs SCE). While in neutral and basic solutions without NH_4^+, the dominant species changes to MoO_4^{2-}, and accordingly, no reduction peak appears except hydrogen evolution. NH_4^+ plays an important role in MoO_2 electrodeposition. A new current peak appears at −1.25 V (vs SCE) in both acid and basic solutions, which is attributed to the reduction of molybdenum complex. The effects of solution composition and the electrodeposition conditions on the current efficiency were discussed systematically. By optimizing the electrodeposition conditions, the current efficiency can reach up to 51.9%.

Key words: MoO_2; NH_4^+; sodium molybdate; electrodeposition; current efficiency; mechanism

1 Introduction

MoO_2 is a transition metal oxide with high specific capacitance, high conductivity and high catalytic activity, showing promising prospects of application in catalyst [1,2], supercapacitor [3], lithium electrical industry [4−6] and so on. The typical industrial technology of producing MoO_2 is hydrogen reduction of MoO_3 [7]. As known to all, this high temperature process still has many disadvantages, such as expensive equipment and high security risks. Electrochemical reduction was reported as a feasible and attractive way to fabricate metal and compound [8,9]. Compared with hydrogen reduction technology, electrochemical reduction process is more moderate, simpler and lower energy cost [10,11].

Many researchers have paid much attention to the electrochemical fabrication of MoO_2 from aqueous solution [12−15]. Although there have been quite a few successful attempts in both acid and basic solutions, the key factors and reduction mechanism remain unclear. In ammonium molybdate aqueous solution, the reactant MoO_4^{2-} is easily condensed to form complex poly-oxometalates (POMs) and the degree of condensation depends on the level of pH [16−18]. Species distribution studies of $Mo-H_2O$ system show that the dominant species is MoO_4^{2-} at pH>5.5 and [Mo]=0.05 mol/L, while in the pH range of 3.0−5.5, the dominant species becomes $Mo_7O_{24}^{6-}$ [19]. At the same time, the critical pH value for $MoO_4^{2-}-Mo_7O_{24}^{6-}$ transformation varies with the total molybdenum concentration. In summary, both the pH value and the Mo(VI) concentration have a great effect on the degree of condensation. Considering the fact that the reduction process and the final products are closely related with the reaction species, the mechanism study is essential for electrodepositing MoO_2 selectively and efficiently.

In addition, it is noticed that most researchers introduced NH_4^+ into molybdate aqueous solution while no one stated the importance of NH_4^+ [12,13]. In our previous studies, we found that the significant distinction in electrolytes between the systems with and without NH_4^+ exists. So, understanding the effect of NH_4^+ on the electrodeposition and the underlying mechanism is of great importance.

In this work, we aimed to adopt electrochemical technology to prepare MoO_2 and improve the selectivity and current efficiency based on the deep understanding of its reaction mechanism. To achieve this, we studied the electrochemical reduction process by linear sweep

Foundation item: Project (51374185) supported by the National Natural Science Foundation of China
Corresponding author: Guo-qu ZHENG; Tel: +86-576-88320429; E-mail: zhenggq@zjut.edu.cn
DOI: 10.1016/S1003-6326(19)65082-X

voltammetry combined with species distribution diagram and Raman spectrum, FT-IR and XRD characterization. The effects of NH_4^+ concentration, molybdenum concentration and pH value on the current efficiency and compositions of products were investigated systematically. This study may provide a theoretical basis for the efficient preparation of MoO_2 via a green and economic technology.

2 Experimental

2.1 Electrodeposition experiments

All electrolytes were prepared with Na_2MoO_4, $(NH_4)_2SO_4$ and double-distilled water. The pH values of the solutions were adjusted with H_2SO_4 and NaOH. 0.5 mm-thick copper sheet with a exposure area of 3 cm^2 was assembled as cathode, which was polished with abrasive papers and cleaned ultrasonically in ethanol before use.

Electrodeposition of MoO_2 was performed in galvanostatic regime (0.1−3 mA/cm^2) on a commercially available power supply, using the pretreated copper sheet and platinum electrode as cathode and anode, respectively. The electrolytes consisted of 0.01−0.25 mol/L Na_2MoO_4 and 0−1 mol/L $(NH_4)_2SO_4$ in pH range of 3−10.5. The deposition time for all experiments was 2 h and the current efficiencies under different conditions were calculated.

In addition, potentiostatic deposition was conducted to determine the compositions of products under certain cathodic potentials, which was performed in a three-compartment cell on a CHI660C working station by applying copper sheet, platinum electrode and saturated calomel electrode (SCE) as the working, counter and reference electrodes, respectively.

2.2 Electrochemical measurements

Electrochemical tests were performed with a CHI660C electrochemical working station using copper electrode (d2 mm) as working electrode, platinum electrode (20 mm × 20 mm) as counter electrode and the saturated calomel electrode as reference electrode. The linear sweep voltammetry curve was measured in 0.05 mol/L Na_2MoO_4 solutions with or without NH_4^+ at a scan rate of 100 mV/s.

2.3 Characterization

Thermal treatment was conducted for the deposits in argon atmosphere at 450 °C for 2 h, with heating and cooling rates of 10 °C/min. The Raman spectra were measured on a micro-Raman system (Renishaw, in via). The FT-IR spectrum measurement was performed on a Nicolet 6700/Thermo/America Fourier transform infrared spectroscope. X-ray diffraction (XRD) patterns of the samples were recorded on a Panalytical X′Pert PRO equipped with Cu K_α radiation (λ=0.15406 nm) at 40 kV and 40 mA. Microstructure observation was carried out by a scanning electron microscope (SEM, FEI Nova Nano SEM 450).

3 Results and discussion

3.1 Electroreduction mechanism in molybdate solution

Typical linear sweep voltammetry (LSV) curves of copper electrode in sodium molybdate solution are shown in Fig. 1(a). It is observed that a strong reduction

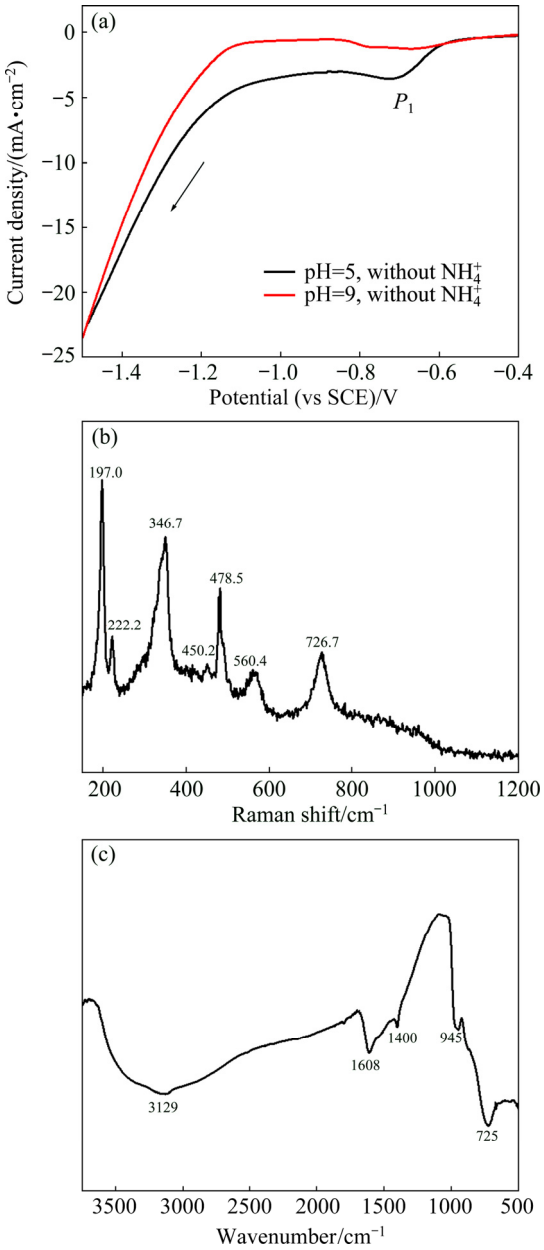

Fig. 1 LSV curves of copper electrode in 0.05 mol/L Na_2MoO_4 solutions with different pH values (a) and corresponding Raman (b) and FT-IR (c) spectra of products prepared by potentiostatic deposition at −0.7 V and pH=5.0

peak emerges at around −0.7 V in the solution of pH 5, while this peak almost disappears in the solution of pH 9. The obvious difference in cathodic process between acid and alkaline media may be ascribed to the variation of dominant species. In light of species distribution diagram [19], we can easily find that the dominant species is MoO_4^{2-} at pH 9 and $Mo_7O_{24}^{6-}$ at pH 5. Therefore, the current peak at −0.7 V should correspond to the reduction of $Mo_7O_{24}^{6-}$, while MoO_4^{2-} must be difficult to reduce as evidenced by the tiny reduction current in this case.

Figures 1(b) and (c) show the Raman and FT-IR spectra of product prepared by potentiostatic deposition in solution of pH 5 at −0.7 V. The product shows seven Raman bands at 197.0, 222.2, 346.7, 450.2, 478.5, 560.4 and 726.7 cm^{-1}. The Raman bands at 560.4 and 726.7 cm^{-1} are attributed to the stretching vibration of Mo—O (I) and Mo—O (II) groups, respectively [20]. In comparison with the Raman bands of the commercial monoclinic 3D MoO_2 powder, the Raman bands of the prepared product are shifted to lower frequencies, which may result from different lattices and inner stress [21]. In FT-IR spectra, five characteristic peaks at 725, 945, 1400, 1608 and 3129 cm^{-1} are observed. The absorption peak at 1608 cm^{-1} is caused by H—O—H bond, while the peak 1400 cm^{-1} is attributed to the vibration of Mo—OH bond [22]. The broad absorption peak at 3000−3500 cm^{-1} is caused by adsorbed water or the —OH groups linked to the films [14]. The peak at about 945 cm^{-1} is the characteristic of Mo═O bond in MoO_2, and the peak at about 725 cm^{-1} is the characteristic of O—Mo—O bond [14,23]. FT-IR spectrum suggests that the product is hydrous molybdenum(IV) oxides, that is, the current peak at −0.7 V denotes the reduction of $Mo_7O_{24}^{6-}$ to molybdenum(IV) oxides.

Figure 2(a) presents the linear sweep voltammetry curves of copper electrode in sodium molybdate solutions with the addition of NH_4^+. Analogously, a current peak denoting the reduction of $Mo_7O_{24}^{6-}$ to molybdenum(IV) oxides appears at around −0.7 V in solution of pH 5. In addition, a new current peak emerges at more negative potential (−1.2 to −1.3 V), whether in the acid solution or in the alkaline solution. The new peak means the occurrence of a new redox reaction, which is probably related with the reduction of molybdenum ammonium complex. In the meantime, from Fig. 2(a) it can be seen that the hydrogen evolution potential on copper is about −0.99 V in 0.025 mol/L $(NH_4)_2SO_4$ solution (pH=5.3), so the reduction of molybdenum ammonium complex happens in the potential range of hydrogen evolution. Thus, the competition with hydrogen evolution will inevitably lead to the decline in current efficiency.

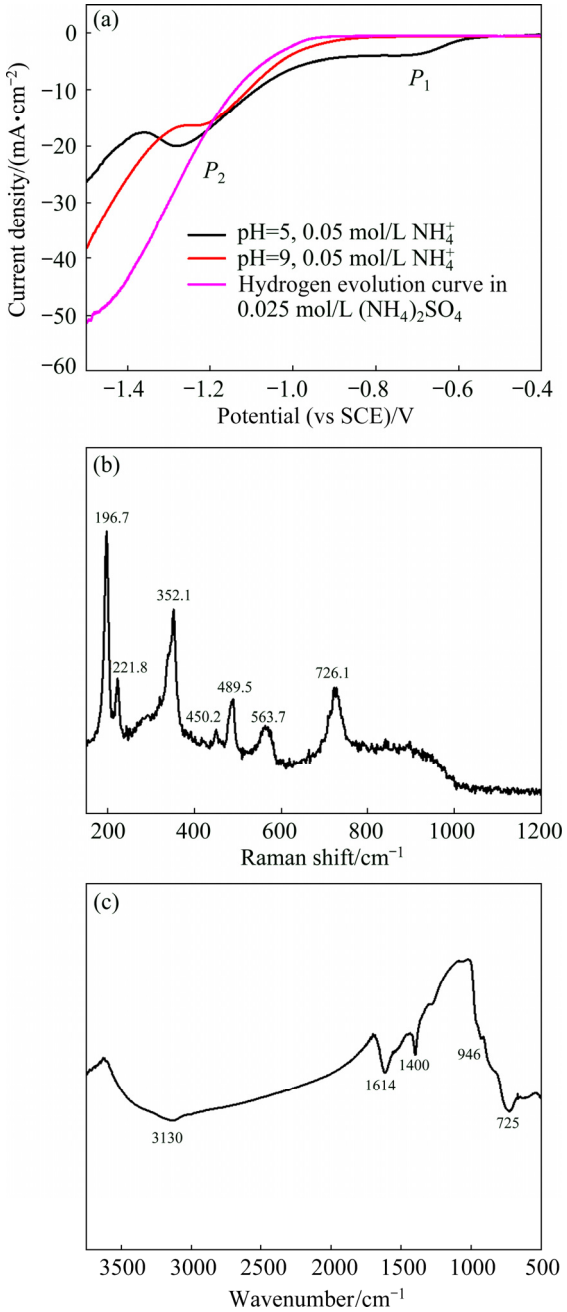

Fig. 2 LSV curves of copper electrode in 0.05 mol/L Na_2MoO_4 + 0.05 mol/L NH_4^+ solutions at different pH values (a) and corresponding Raman (b) and FT-IR (c) spectra of products prepared by potentiostatic deposition at −1.2 V and pH=9.0

Raman and FT-IR spectra of the sample potentiostaticaly deposited from solution with NH_4^+ at −1.2 V and pH=9.0 are displayed in Figs. 2(b) and (c), respectively. Similar to the product deposited at −0.7 V, the product at −1.2 V yields seven Raman bands at 196.7, 221.8, 352.1, 450.2, 489.5, 563.7 and 726.1 cm^{-1}, and the FT-IR spectra suggests that the product is composed of hydrous molybdenum(IV) oxides. Both the Raman and FT-IR spectra indicate that the reaction at

−1.2 V corresponds to the reduction of molybdenum ammonium complex to molybdenum(IV) oxides.

The phase structures of the products electrodeposited at −0.7 and −1.2 V were further analyzed by XRD pattern (Fig. 3). It is found that for the samples without annealing, no characteristic diffraction peak was observed besides the diffraction peak of Cu substrate. However, when the two samples were annealed in argon atmosphere, characteristic diffraction peaks denoting the monoclinic MoO_2 (JCPDS01−078−1071) emerged at 2θ values of 25.9°, 36.7° and 53°. This result reveals that the product, whether prepared at −0.7 V or −1.2 V, has an amorphous structure, and high crystallinity of monoclinic MoO_2 can be obtained after annealing.

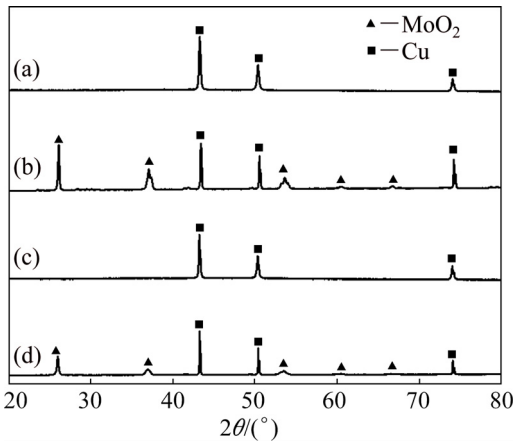

Fig. 3 XRD patterns of products deposited at −0.7 V in 0.05 mol/L Na_2MoO_4 (pH=5.0) without (a) and with (b) heat treatment at 450 °C for 2 h in argon, and products deposited at −1.2 V in solution with 0.05 mol/L Na_2MoO_4 and 0.05 mol/L NH_4^+ (pH=9.0) without (c) and with (d) heat treatment at 450 °C for 2 h in argon

Figure 4 shows the voltammetric curves of samples measured in aqueous solutions with different pH values and different Mo(VI) concentrations. It is observed that in the case of 0.05 mol/L Mo(VI), the cathodic peak P_1 related to the reduction of $Mo_7O_{24}^{6-}$ to molybdenum(IV) oxides becomes weaker with the increase of solution pH value and almost disappears at pH=5.5. However, when the Mo(VI) concentration is 0.5 mol/L, the critical pH for the emergence of peak P_1 increases to 6.5. The variation of peak P_1 with pH value and Mo(VI) concentration may be related with the change of main species in solution. According to the species distribution diagram [19], it is clear that the main existence region of $Mo_7O_{24}^{6-}$ is in the range of pH<5.5 for the case of 0.05 mol/L Mo(VI), so peak P_1 weakens and tends to disappear with pH increasing due to the reduction of reactants. While in the condition of higher Mo(VI) concentration (0.5 mol/L), the main existence pH region of $Mo_7O_{24}^{6-}$ expands towards high pH region (<6.5), as a result, the reduction reaction of molybdenum(IV) oxides can occur at higher pH value. In addition, it is noted that the current peak P_1 has a broad trend, which is likely caused by the coreduction of multiple polymeric species, such as $Mo_7O_{24}^{6-}$, $HMo_7O_{24}^{5-}$, $H_2Mo_7O_{24}^{4-}$ and $H_3Mo_7O_{24}^{3-}$.

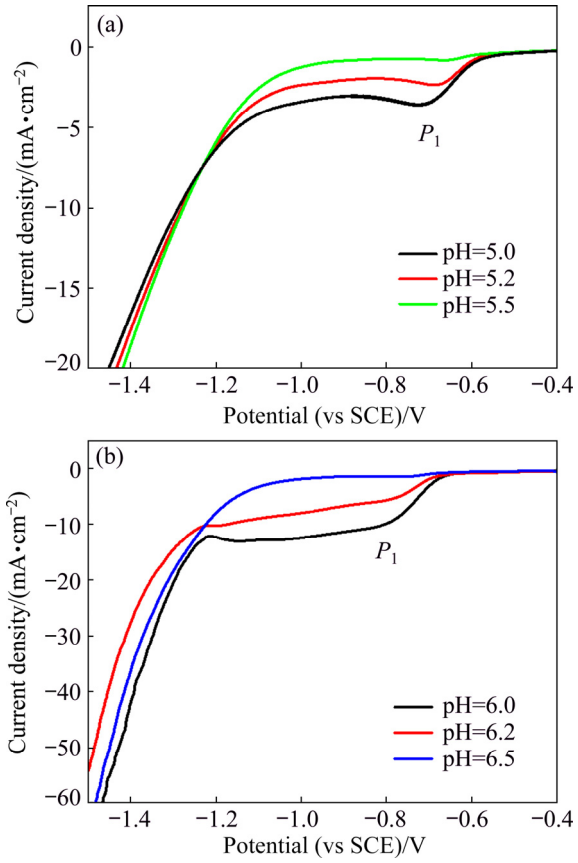

Fig. 4 LSV curves of copper electrode in aqueous solutions with 0.05 mol/L Na_2MoO_4 (a) and 0.5 mol/L Na_2MoO_4 (b) at different pH values

Effects of NH_4^+ concentration on molybdenum(IV) oxides reduction are shown in Fig. 5. The Raman and FT-IR analyses above have confirmed that both current peaks P_1 and P_2 correspond to the reduction of molybdenum(IV) oxides, while their reactants are different. It is found that peak P_1 is slightly affected by the NH_4^+ concentration. On the contrary, peak P_2 becomes stronger with increasing NH_4^+ concentration. These results further prove that the reduction peak P_2 is closely related with the molybdenum ammonium complex. Particularly, in neutral or basic conditions, the main species MoO_4^{2-} binds to NH_4^+ to form $(NH_4)_2MoO_4$, which adheres on the electrode surface and is then reduced to molybdenum(IV) oxides. In faintly acidic conditions, a depolymerization process of paramolybdate $(NH_4)_6Mo_7O_{24}\cdot 4H_2O$ to the simple molybdate $(NH_4)_2MoO_4$ takes place firstly [24], and then surfactant $(NH_4)_2MoO_4$ is reduced to molybdenum(IV) oxides. Therefore, the higher the NH_4^+ concentration is, the

more the $(NH_4)_2MoO_4$ is produced, which is advantageous to the deposition of molybdenum(IV) oxides.

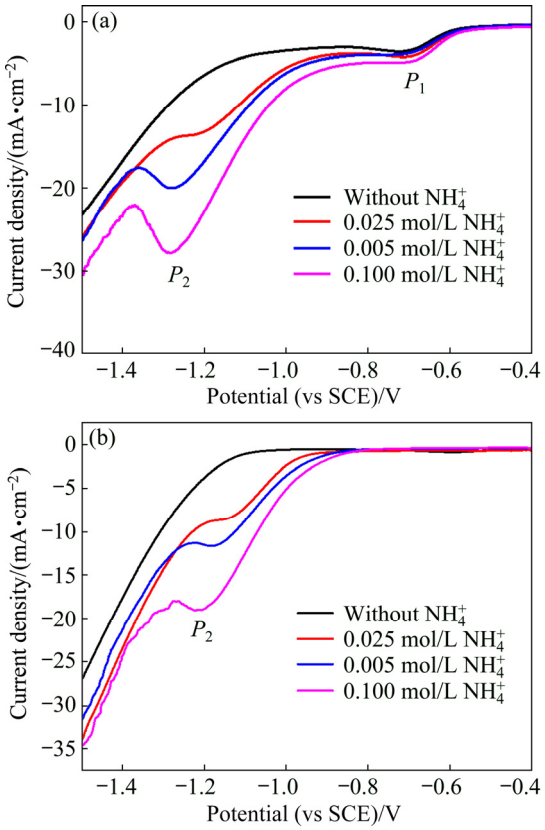

Fig. 5 LSV curves of copper electrode in aqueous solutions with different NH_4^+ concentrations at pH=5.0 (a) and pH=9.0 (b)

Figure 6 shows the LSV curves of copper electrode in molybdate solution at different temperatures. It is found that the potentials of peaks P_1 and P_2 shift positively and the peak current densities are enhanced gradually with increasing the temperature, i.e. an acceleration effect on the reduction of molybdenum(IV) oxides can be obtained by increasing temperature.

3.2 Electrodeposition of molybdenum(IV) oxides

The current efficiency and the quality of electrodeposits are the major concerns in electrodeposition. So, electrodeposition experiments were conducted to investigate the effects of solution composition and the electrodeposition conditions such as current density and temperature, based on which an optimum technology to prepare MoO_2 was proposed.

3.2.1 Effects of pH and NH_4^+ concentration

Figure 7 shows the current efficiency varying with the solution pH and NH_4^+ concentration. In the case without NH_4^+, high current efficiency (>50%) can be obtained at pH<5.5 and almost no product generated at pH>6, which is consistent with the mechanism study, i.e., the reducible species $Mo_7O_{24}^{6-}$ only exists in acid solution. When NH_4^+ is introduced into the electrolyte, the concentration of reactant $Mo_7O_{24}^{6-}$ will decrease in the range of pH<5.5; meanwhile, a new reactant, molybdenum ammonium complex will form. The LSV study has indicated that the reduction of $Mo_7O_{24}^{6-}$ happens at about −0.7 V, while the reduction of molybdenum ammonium complex occurs at about −1.2 V accompanied with hydrogen evolution, so naturally, the current efficiency in acid solution declines by the addition of NH_4^+. However, in neutral and basic conditions, no other species except molybdenum ammonium complex can be reduced to molybdenum(IV) oxides, as a result, the current efficiency increases in the presence of NH_4^+.

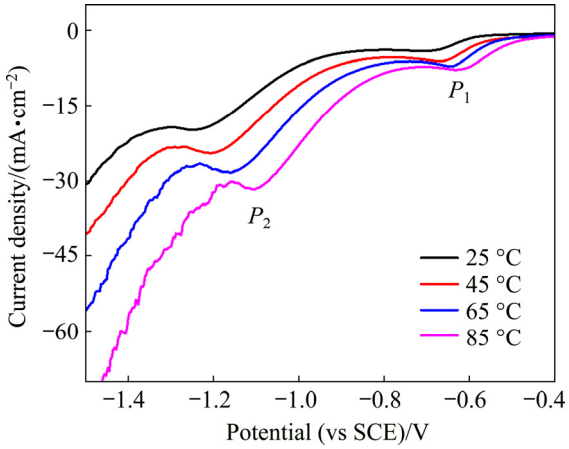

Fig. 6 LSV curves of copper electrode in aqueous solution containing 0.05 mol/L NH_4^+ and 0.05 mol/L Na_2MoO_4 at pH=5.0 and different temperatures

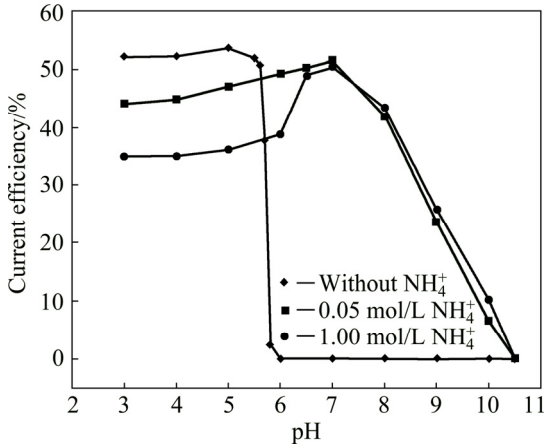

Fig. 7 Cathodic current efficiency of deposits prepared at different solution pH and NH_4^+ concentrations over 12 h deposition (J=1 mA/cm^2, t=30 °C, [Mo]=0.05 mol/L)

In addition, molybdenum blue was observed at pH<3 in our experiments, which is likely resulted from the reduction of new species such as $Mo_8O_{24}^{4-}$ [25]. It is proved that this condition is disadvantageous for the

deposition of molybdenum(IV) oxides.

In general, the current efficiency increases gradually with increased pH in acid condition and reaches the maximum at pH=7.0 in the presence of NH_4^+, after which it declines rapidly. The pH range suitable for the preparation of molybdenum(IV) oxides is enlarged by the addition of NH_4^+ although there is a slight decline in current efficiency in acid conditions. Therefore, to a certain degree, the addition of NH_4^+ is beneficial to the electrodeposition of molybdenum(IV) oxides.

Figure 8 shows the microstructure of the electrodeposits prepared at current density of 1 mA/cm^2 for 2 h in solutions with 0.05 mol/L Mo(VI), 1 mol/L NH_4^+ and different pH values. Deep fissures were observed on the surface of electrodeposits prepared in solutions with pH values of 5.0 and 7.0, showing high stripping tendency. However, for the case of pH=9.0, the electrodeposits are more compact, the cracks are decreased and many small tumors are packed on the surface. Therefore, the product is difficult to strip off , which is not beneficial to the fabrication of MoO_2 powder.

Prior studies indicated that the electrodeposits were composed of hydrous molybdenum(IV) oxides, which can be transferred to monoclinic MoO_2 after annealing. So, heat treatment was performed in dry argon at 450 °C for 2 h and the microstructures of the resultant products are presented in Fig. 9. From Fig. 9, we can find that the products deposited at pH=5.0 and pH=7.0 are dehydrated and converted into granular structure. The granular particles with particle size ranged from 50 to 200 nm are uniformly and loosely distributed on the surface. Similarly, the products deposited at pH=9.0 are also converted into granular structure, but the particles are

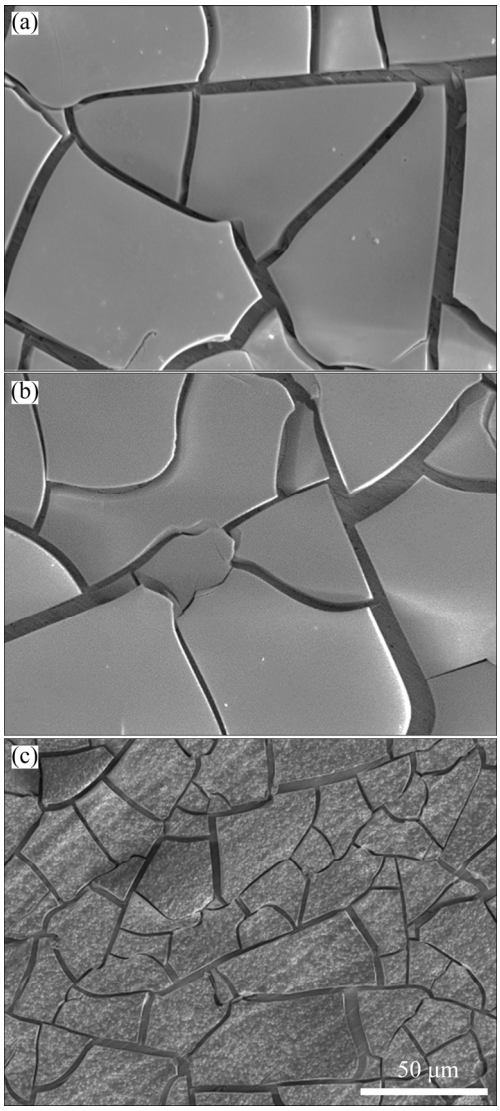

Fig. 8 SEM images of deposits prepared at constant current density of 1 mA/cm^2 for 2 h from solutions with 0.05 mol/L Mo(VI), 1 mol/L NH_4^+ and different pH values: (a) pH=5.0; (b) pH=7.0; (c) pH=9.0

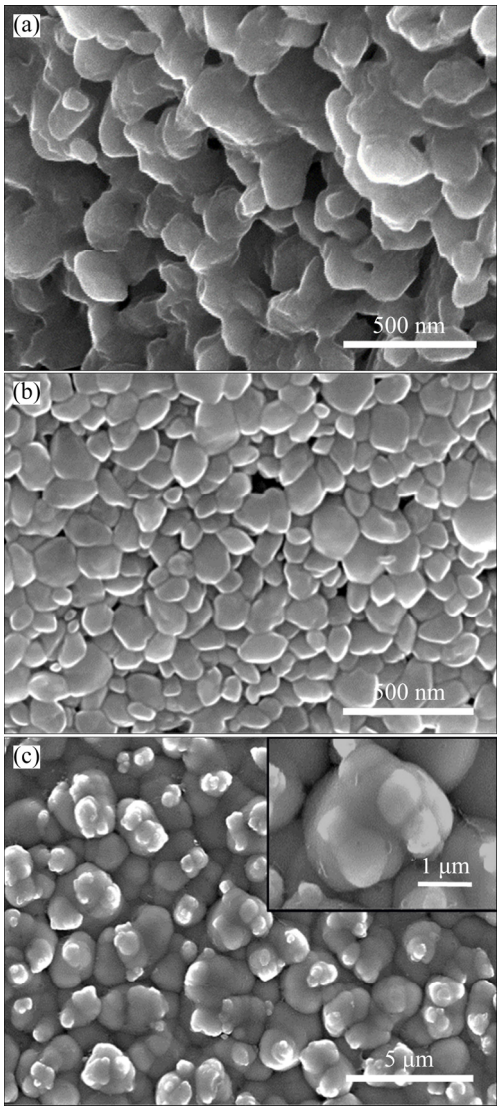

Fig. 9 SEM images of annealed electrodeposits prepared at constant current density of 1 mA/cm^2 for 2 h from solutions with 0.05 mol/L Mo(VI) and 1 mol/L NH_4^+ at different pH values: (a) pH=5.0; (b) pH=7.0; (c) pH=9.0

compact and irregular with many small tumors packed on the surface. So, the favorable pH range to fabricate regular MoO_2 particles is pH<7.0 under the addition of NH_4^+.

3.2.2 Effect of current density

Figure 10 shows the cathodic current efficiency of MoO_2 deposition at different current densities. It is observed that the current efficiency is lowered by increasing the current density. Specifically, the current efficiency is up to 54.3% at 0.1 mA/cm^2, and reduces to 14.5% at 4 mA/cm^2. The dramatic decline in current efficiency is mainly due to the severe hydrogen evolution reaction at high current density. From the SEM images of deposits after annealing (shown in Figs. 9 and 11), we can find that the surface morphology is greatly influenced by the current density. The particle size decreases as the current density increases from 1 to 3 mA/cm^2. As we know, on one hand the high current density accelerates the nucleation; thus leads to the formation of fine crystals. On the other hand, hydrogen evolution also has grain refinement effect. In general, the appropriate current density is around 1 mA/cm^2, by which both the deposition speed and current efficiency are high and simultaneously, the particle size meets the requirement.

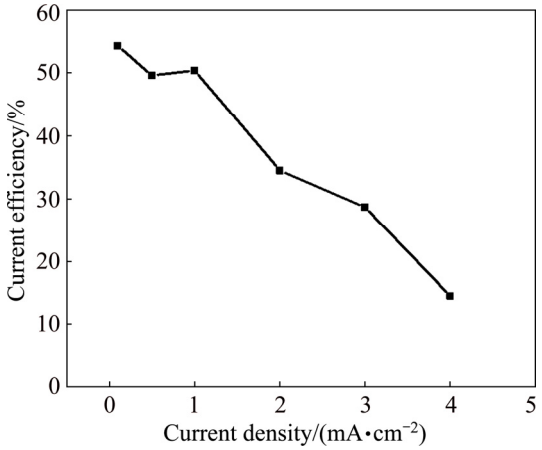

Fig. 10 Cathodic current efficiency of deposits prepared at different current densities for 2 h (t=30 °C, [Mo]=0.05 mol/L, [NH_4^+]=1 mol/L, pH=7.0)

3.2.3 Effect of Mo(VI) concentration

Figure 12 shows the cathodic current efficiency of MoO_2 deposition on Mo(VI) concentration. It indicates that the increase of Mo(VI) concentration leads to low current efficiency. At low Mo(VI) concentrations (0.01 and 0.05 mol/L), the current efficiency is higher than 50%, while at high Mo(VI) concentration (0.25 mol/L), current efficiency is decreased to ~35.7%, which may be caused by the harmful side reaction (for instance, Mo(V) reduction) occurring during cathodic electrodeposition process. The side reaction competes with the deposition of MoO_2 and it seems that the increase of Mo(VI) concentration facilitates the occurrence of side effects. Therefore, for the production efficiency, 0.05 mol/L Mo(VI) is the most suitable condition for MoO_2 deposition.

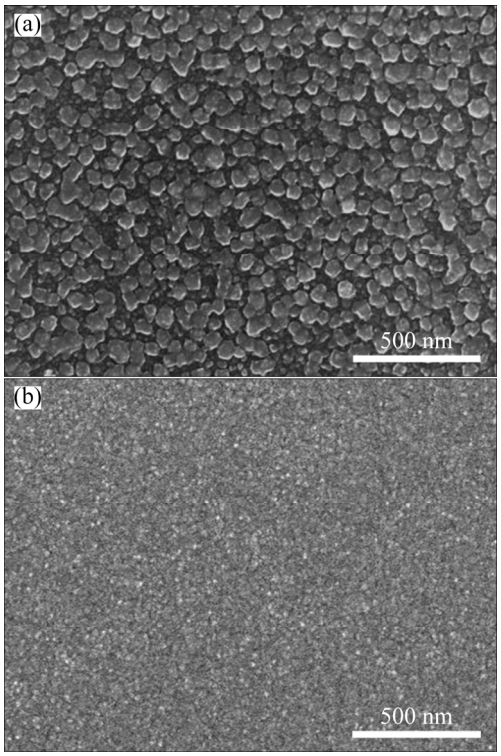

Fig. 11 SEM images of annealed deposits prepared at pH=7.0 and different current densities for 2 h from solutions with 0.05 mol/L Mo(VI) and 1 mol/L NH_4^+: (a) 2 mA/cm^2; (b) 3 mA/cm^2

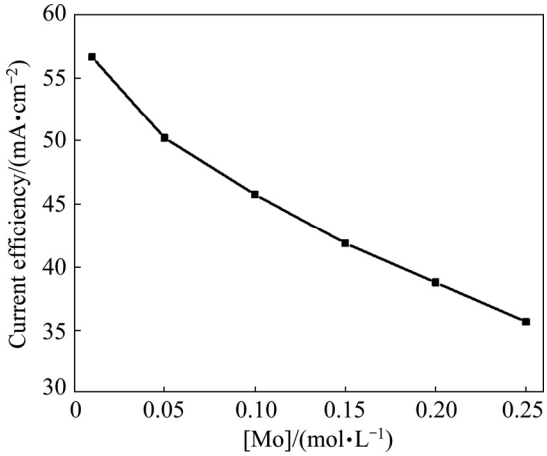

Fig. 12 Cathodic current efficiency of deposits prepared at different Mo(VI) concentrations for 2 h (J=1 mA/cm^2, t=30 °C, [NH_4^+]=1 mol/L, pH=7.0)

3.2.4 Effect of temperature

The effect of temperature on the current efficiency of MoO_2 deposition is presented in Fig. 13. It is shown that when the temperature rises from 10 to 70 °C, the

current efficiency is reduced slightly from 51.9% to 43.4%. From the LSV study we know that the increase of temperature has an acceleration effect on the reduction of molybdenum (IV) oxides. However, hydrogen evolution reaction is also promoted by increasing temperature. So the competition of these two reactions leads to a slight declination in current efficiency. On the other hand, temperature is an important parameter affecting complexation equilibrium. In most cases, low temperature is conducive to the formation of complexes. Therefore, the main reactant, i.e., molybdenum ammonium complex, may depolymerize at higher temperatures, thus resulting in the declination of current efficiency. Therefore, low temperature is favorable for MoO_2 deposition.

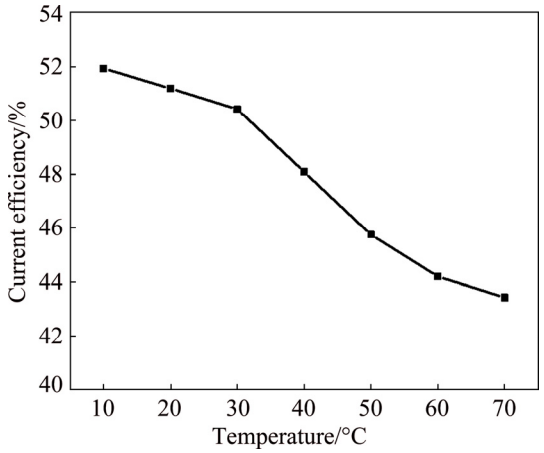

Fig. 13 Cathodic current efficiency of deposits prepared at different temperatures for 2 h (J=1 mA/cm^2, [Mo]= 0.05 mol/L, [NH_4^+]=1 mol/L, pH=7.0)

4 Conclusions

(1) The electrochemical reduction mechanism of MoO_2 from ammonium molybdate electrolyte was revealed. There exist two reducible species in this system, i.e., $Mo_7O_{24}^{6-}$ and molybdenum ammonium complex. Only $Mo_7O_{24}^{6-}$ exists in weak acid solutions with reduction peak potential around −0.7 V (vs SCE). Molybdenum ammonium complex exists in both acid and basic solutions, while its reduction occurs at more negative potentials (from −1.2 to −1.3 V, vs SCE) accompanied with hydrogen evolution. So, the competition with hydrogen evolution will inevitably lead to the decline in current efficiency.

(2) Current efficiency, structure and composition of MoO_2 are greatly dependent on the solution composition and the electrolytic conditions. Loose and easily stripping deposits can be obtained in baths with 1 mol/L NH_4^+ and 0.05 mol/L Mo(VI) at pH=7.0. By optimizing electrodeposition parameters, current efficiency can be as high as 51.9%.

(3) Electrodeposited amorphous molybdenum (IV) oxides can be transferred to uniform and nanometer-size crystalline MoO_2 by annealing in dry argon at 450 °C. This work thus hopefully provides a new strategy for the industrial preparation of MoO_2 powder.

References

[1] ZHOU Wei-jia, HOU Dong-man, SANG Yuan-hua, YAO Shu-hua, ZHOU Jian, LI Guo-qiang, LI Li-gui, LIU Hong, CHEN Shao-wei. MoO_2 nanobelts@nitrogen self-doped MoS_2 nanosheets as effective electrocatalysts for hydrogen evolution reaction [J]. Journal of Materials Chemistry A, 2014, 2(29): 11358−11364.

[2] BERG F G A V D, GLEZER J H E, SACHTLER W M H. The role of promoters in COH_2 reactions: Effects of MnO and MoO_2, in silica-supported rhodium catalysts [J]. Journal of Catalysis, 1985, 93(2): 340−352.

[3] RAJESWARI J, KISHORE P S, VISWANATHAN B, VARADARAJAN T K. One-dimensional MoO_2 nanorods for supercapacitor applications [J]. Electrochemistry Communications, 2009, 11(3): 572−575.

[4] LUO Wei, HU Xiao-luo, SUN Yong-ming, HUANG Yun-hui. Electrospinning of carbon-coated MoO_2 nanofibers with enhanced lithium-storage properties [J]. Physical Chemistry Chemical Physics, 2011, 13(37): 16735−16740.

[5] FU Hao, XU Zhan-wei, WANG Tian, LI Kang, SHEN Xue-tao, LI Jia-yin, HUANG Jian-feng. Rate behavior of MoO_2/graphene oxide lithium-ion battery anodes from electrochemical contributions [J]. Journal of the Electrochemical Society, 2018, 165(3): A439−A447.

[6] CHRISTIAN P A, CARIDES J N, DISALVO F J, WASZCZAK J V. Molybdenum oxide cathodes in secondary lithium cells [J]. Journal of the Electrochemical Society, 1980, 127(11): 2315−2319.

[7] HU Bin, MAI Li-qiang, CHEN Wen, YANG Fan. From MoO_3 nanobelts to MoO_2 nanorods: Structure transformation and electrical transport [J]. ACS Nano, 2009, 3(2): 478−482.

[8] NIU Te, CHEN Wei-wei, WANG Lu. Crain growth and thermal stability of nanocrystalline Ni−TiO_2 [J]. Transactions of Nonferrous Metals Society of China, 2017, 27(10): 2300−2309.

[9] WU Lian-kui, WANG Wei-ke, CAO Hua-zhen, HOU Guang-ya, TANG Yi-ping, ZHENG Guo-qu. Electrodeposition of bright nickel from liquid ammonia solution containing chloride [J]. Journal of the Electrochemical Society, 2016, 163(14): D829−D835.

[10] CAO Hua-zhen, CHAI Da-gan, WU Lian-kui, ZHENG Guo-qu. Communication — A mechanistic study on electrodeposition of rhenium from acidic solution of ammonium perrhenate [J]. Journal of the Electrochemical Society, 2017, 164(13): D825−D827.

[11] ZHOU Ya-ru, ZHANG Shan, NIE Lin-lin, ZHU Ze-jie, ZHANG Jian-qing, CAO Fa-he, ZHANG Jun-xi. Electrodeposition and corrosion resistance of Ni−P−TiN composite coating on AZ91D magnesium alloy [J]. Transactions of Nonferrous Metals Society of China, 2016, 26(11): 2976−2987.

[12] ZACH M P, INAZU K, NG K H, HEMMINGER J C, PENNER R M. Synthesis of molybdenum nanowires with millimeter-scale lengths using electrochemical step edge decoration [J]. Chemistry of Materials, 2002, 14(7): 3206−3216.

[13] BANICA R, BARVINSCHI P, VASZILCSIN N, NYARI T. A comparative study of the electrochemical deposition of molybdenum oxides thin films on copper and platinum [J]. Journal of Alloys and Compounds, 2009, 483(1): 402−405.

[14] PATIL R S, UPLANE M D, PATIL P S. Structural and optical properties of electrodeposited molybdenum oxide thin films [J]. Applied Surface Science, 2006, 252(23): 8050−8056.

[15] WANG Fan, LU Bing-qiang. Well-aligned MoO_2 nanowires arrays:

Synthesis and field emission properties [J]. Physica B Condensed Matter, 2009, 404(14): 1901−1904.

[16] ZHANG Jia-Liang, ZHAO Zhong-wei. Thermodynamic analysis for separation of tungsten and vanadium in W(VI)−V(V)−H_2O system [J]. The Chinese Journal of Nonferrous Metals, 2014, 24(6): 1656−1662. (in Chinese)

[17] KRISHNAN C V, GARNETT M, HSIAO B, CHU B, Electrochemical measurements of isopolyoxomolybdates. 1: pH dependent behavior of sodium molybdate [J]. International Journal of Electrochemical Science, 2007, 2(1): 29−51.

[18] TYTKO K H, BAETHE G, CRUYWAGEN J J. Equilibrium studies of aqueous polymolybdate solutions in 1 M sodium chloride medium at 25 °C [J]. Inorganic Chemistry, 1985, 24(20): 3132−3136.

[19] ZHANG Jia-liang, ZHAO Zhong-wei, CHEN Xin-yu, LIU Xu-heng. Thermodynamic analysis for separation of tungsten and molybdenum in W−Mo−H_2O system [J]. The Chinese Journal of Nonferrous Metals, 2013, 23(5):1463−1470. (in Chinese)

[20] DIETERLE M, MESTL G. Raman spectroscopy of molybdenum oxides. Part II: Resonance Raman spectroscopic characterization of the molybdenum oxides Mo_4O_{11} and MoO_2 [J]. Physical Chemistry Chemical Physics, 2002, 4(5): 822−826.

[21] KUMARI L, MA Y R, TSAI C C, LIN Y W, WU S Y, CHENG K W, LIOU Y. X-ray diffraction and Raman scattering studies on large-area array and nanobranched structure of 1D MoO_2 nanorods [J]. Nanotechnology, 2007, 18(11): 115717.

[22] JUDEINSTEIN P, MORINEAU R, LIVAGE J. Electrochemical degradation of $WO_3 \cdot nH_2O$ thin films [J]. Solid State Ionics, 1992, 51(3−4): 239−247.

[23] NIJOLĖ D, DOVILĖ S. Photoelectrochemical properties of MoO_2 thin films [J]. Journal of Solid State Electrochemistry, 2013, 17(4):1175−1184.

[24] CLAYTON C R, LU Y C. Electrochemical and XPS evidence of the aqueous formation of Mo_2O_5 [J]. Surface and Interface Analysis, 2010, 14(1−2): 66−70.

[25] CLAUSEN D F, SHROYER J H. Molybdenum blue reaction [J]. Analytical Chemistry, 1948, 20(10): 925−926.

从钼酸铵溶液中电沉积 MoO_2 的机理

曹华珍，童程剑，张惠斌，郑国渠

浙江工业大学 材料科学与工程学院，杭州 310014

摘　要：采用线性扫描伏安曲线、物种分配图、拉曼光谱、傅里叶红外光谱、X 射线衍射等手段研究从酸性和碱性体系中电沉积 MoO_2 的机理。结果表明，钼酸铵电解液中主要存在两种可被还原的物种，即 $Mo_7O_{24}^{6-}$ 和钼铵络合物。在不含 NH_4^+ 的弱酸性体系中，主要物种为 $Mo_7O_{24}^{6-}$，其还原为 Mo(IV) 氧化物的峰电位约为−0.7 V (vs SCE)；在不含 NH_4^+ 的中性和碱性体系中，主要物种为 MoO_4^{2-}，此时扫描伏安曲线中无还原峰出现，仅发生析氢反应；电解体系中加入 NH_4^+ 对 MoO_2 电沉积产生重要影响，酸性或碱性条件下均在−1.25 V (vs SCE)处出现一个新的还原峰，对应于钼铵络合物的还原。本文作者系统地研究电解液组分和电沉积条件的影响。通过优化电沉积条件，电流效率达到 51.9%。

关键词：MoO_2；NH_4^+；钼酸钠；电沉积；电流效率；机理

(Edited by Wei-ping CHEN)